Changes in Dissolved Organic Matter during the Treatment Processes of a Drinking Water Plant in Sweden and Formation of Previously Unknown Disinfection Byproducts

Michael Gonsior, Philippe Schmitt-Kopplin, Helena Stavklint, Susan D. Richardson, Norbert Hertkorn and David Bastviken

Gonsior, M., Schmitt-Kopplin, P., Stavklint, H., Richardson, S. D., Hertkorn, N., Bastviken, D., (2014), Changes in Dissolved Organic Matter during the Treatment Processes of a Drinking Water Plant in Sweden and Formation of Previously Unknown Disinfection Byproducts, *Environmental Science and Technology*, 48(21), 12714-12722. https://doi.org/10.1021/es504349p

Original publication available at:
https://doi.org/10.1021/es504349p

Dissolved Organic Matter Changes along Treatments of a Drinking Water Plant in Sweden and the Formation of Previously Unknown DBPs

Michael Gonsior [a*], *Philippe Schmitt-Kopplin* [b,c], *Helena Stavklint* [d], *Susan D. Richardson* [e], *Norbert Hertkorn* [b] *and David Bastviken* [f]

[a] University of Maryland Center for Environmental Science, Chesapeake Biological Laboratory, Solomons, USA

[b] Helmholtz Zentrum München, Analytical BioGeoChemistry, Neuherberg, Germany

[c] Technische Universität München, Analytical Food Chemistry, D-85354 Freising-Weihenstephan, Germany

[d] Tekniska verken i Linköping AB, Sweden

[e] University of South Carolina, Department of Chemistry and Biochemistry, Columbia, SC, USA

[f] Linköping University, Department of Thematic Studies – Environmental Change, Linköping, Sweden

[*]Corresponding author. phone: +14103267245, fax: +14103267302 Email address: gonsior@umces.edu

Keywords: ultrahigh resolution mass spectrometry, FT-ICR-MS, disinfection by-products, DBPs, drinking water treatment, dissolved organic matter, DOM, nuclear magnetic resonance, NMR

Abstract

The changes in dissolved organic matter (DOM) throughout the treatment processes in a drinking water treatment plant in Sweden and the formation of disinfection by-products (DBPs) were evaluated by using ultrahigh resolution mass spectrometry (resolution ~ 500,000 at *m/z* 400) and nuclear magnetic resonance (NMR). Mass spectrometric results revealed that flocculation induced substantial changes in the DOM and caused quantitative removal of DOM constituents that usually are associated with DBP formation. While half of the chromophoric DOM (CDOM) was removed by flocculation, about 4-5 mg L^{-1} total organic carbon remained in the finished water. A conservative approach revealed the formation of about 800 mass spectrometry ions with unambiguous molecular formula assignments that contained at least one halogen atom. These molecules likely represented new DBPs, which could not be prevented by the flocculation process. The most abundant *m/z* peaks, associated with formed DBPs, could be assigned to $C_5HO_3Cl_3$, $C_5HO_3Cl_2Br$ and $C_5HO_3ClBr_2$ by using isotope simulation patterns with the likely DBPs were produced and suggested the presence of halogenated polyphenolic and aromatic acid-type structures, which was supported by possible structures that matched the lower molecular mass range (max. 10 carbon atoms) of these DBPs. ^{1}H-NMR before and after disinfection revealed about a 2% change of the overall ^{1}H-NMR signals supporting a significant change of the DOM caused by disinfection. This study underlines that a large and increasing number of people are exposed to a very diverse pool of organohalogens through water - by both drinking and uptake through the skin upon contact. Non-target analytical approaches are indispensable to reveal the magnitude of this exposure and to test alternative ways to reduce it.

Introduction

Disinfection of drinking water is widely implemented to avert diseases by infectious water-borne pathogens. Disinfection is accomplished with strong oxidants, such as free chlorine, chlorine dioxide, chloramines and ozone, which efficiently kill pathogens. It was not until the 1970s when the first group of disinfection by-products (DBPs) were discovered [1] and related to adverse health effects (i.e., cancer) [2]. These secondary chemicals are formed by the reaction of the disinfectant with natural dissolved organic matter (DOM) or other micro-pollutants, such as bromide and iodide.

Since that time, a wealth of information has been produced about DBPs and their toxicity, including cytotoxicity, genotoxicity, and adverse birth outcomes [3-17]. More than 600 DBPs have now been identified [9]. However, about a 50% decrease of free chlorine (HOCl) remains unaccounted for during drinking water treatment and cannot be entirely explained by known DBPs [11, 18]. It has long been suggested that free chlorine gets incorporated into high molecular weight DOM, and early research on molecular size fractions indicated that more than 50% of the total organic halogen formed in chlorinated drinking water is greater than 1000 Da [19-21]. Recent research using ultrahigh resolution mass spectrometry, which has the ability to track the incorporation of chlorine in extremely complex mixtures of organic molecules in drinking water, confirmed the presence of high molecular weight chlorinated DBPs [22, 23], although all ions found were well below 1000 Da. This discrepancy between the earlier membrane fractionation experiments and the more recent ultrahigh resolution mass spectrometry experiments may be due to the fact that not covalently bound aggregates remain intact during membrane size fractionations, but separate in electrospray ionization with ultrahigh resolution mass spectrometry. A previous suggestion that multiply charged ions are responsible for the

much lower mass range observed in mass spectrometry when compared to size exclusion chromatography interfaced with ultraviolet detectors [24] can be ruled out, because of the very precise measurements of masses in this study that have an error much less than the mass of an electron. Here, multiply-charged ions, which occupy the space in-between nominal mass clusters of singly charged ions, were largely absent.

A large number of DBPs have been identified, but the abundance, exposure, and toxicity of these complex mixtures are only slowly emerging. Despite the expected complex formation mechanisms of DBPs, the United States and Europe regularly monitor only three classes: trihalomethanes (THMs), haloacetic acids (HAAs) and oxyhalides (bromate and chlorite) [25, 26]. Our knowledge about DBP toxicity and abundance thus remains limited. Notably, the extensive molecular diversity of DBPs makes it very difficult to identify specific toxic DBPs.

Disinfection is expected to become more important in the future, due to climate change with accompanying increasing temperatures and prolonged warm seasons, which will likely yield higher amounts of waterborne pathogens, particularly in temperate or boreal regions that traditionally had very limited water borne illnesses recorded in the past. Sweden is such an example with 50% of its drinking water coming from surface water sources. In this context, proper assessments of DBP exposure are increasingly important. To what extent removal of DOM before disinfection also removes DBP precursors is critical. Such tests are rare because of difficulties to investigate complex DBP-mixtures incorporated into the large molecular diversity of DOM. The main objective of this study was to follow the complex mixture of DOM entering a water treatment plant throughout the different treatment processes and to characterize the complex pool of DBPs formed. Known classes of DBPs such as HAAs or THMs are either

outside of the mass window or not retained by the solid phase extraction used in this study and therefore were not evaluated in this study.

Methods

Sampling and solid phase extraction (SPE) of DOM. All water samples were collected at the Råberga water treatment plant located in Linköping, Sweden at the same time in august 2011. This plant is a prime example for smaller scale water treatment that faces the challenges in controlling and maintaining high water quality standards. The raw water intake is 2.5 m below the surface of the Stångån River. The water is pumped through a grid into the chemical precipitation unit, which consists of three parallel assemblies, each consisting of a stirred flocculation tank and a three-story sedimentation tank. Aluminum sulfate is used as a flocculant, supplemented with sodium silicate as a flocculation aid. The water passes then through six rapid sand filters at a filter speed of 4-8 $m^3 h^{-1}$ for particle removal. The pH is adjusted to pH 8.4 with sodium hydroxide before the water is pumped to eight slow sand filters, which have a total area of 5,440 m^2 and a filter rate of 0.13 to 0.26 $m^3 h^{-1}$. Further, water pH adjustments are achieved by adding sodium hydroxide. The final step is disinfection with sodium hypochlorite (NaOCl). The annual average concentration of total chlorine before distribution was 0.36 mg L^{-1}. The mixed water is stored in reservoirs totaling 11,000 m^3 before the water is distributed. The treatment plant is designed to produce 10,000 m^3 per day. The Stångån River has relatively high total organic carbon (TOC) concentrations (10-12 mg L^{-1}) and a flocculation treatment was necessary to reduce the CDOM and to reduce the TOC. The treatment plant regularly measured TOC and the variation of TOC in the raw and processed waters between 2011 and 2013 is given in Supporting Information (Fig. S1). The TOC of the raw water averaged 10 mg L^{-1}. Flocculation

removed about half of the TOC and finished water still contained 4-5 mg L^{-1}. Taste and odor problems occurred occasionally and the treatment plant is undergoing major upgrades in 2014.

Duplicate samples of 2 L raw water (intake), 5 L water after flocculation, 5 L after rapid sand filtration, 5 L after slow sand filtration and 5 L after disinfection were collected in acid-base cleaned glass bottles. Immediately after collection, all samples were filtered through pre-combusted Whatman GF/F glass fiber filters and no quenching agents were added to the disinfected water to avoid any additional sources of contamination. The pH was adjusted to 2 using high purity grade formic acid (98%). This step was necessary to enhance the SPE efficiency to about 60% dissolved organic carbon (DOC) using Agilent Bond Elut PPL SPE cartridges filled with 1 g of highly functionalized styrene-divinylbenzene (SDVB) polymer that has been modified with a proprietary non-polar surface. The SPE method has been previously described [27], but we modified it by replacing concentrated HCl with concentrated formic acid to avoid any sampling bias of chloride ions in the methanolic eluent. Chloride ions are problematic, because even at relatively low concentrations, DOM may form chloride adducts that could be mistaken for covalently bound DBPs and were even used as a dopant to analyze saccharides [28]. No chloride adducts were formed in samples collected prior to disinfection in this study confirming the effectiveness using formic acid instead of HCl to avoid adduct formations. The SPE cartridge was activated using methanol (Sigma-Aldrich Chromasolv LC-MS grade methanol), washed with acidified (pH 2) high purity water (Sigma-Aldrich Chromasolv LC-MS grade water). Then, the acidified sample was gravity-fed through the SPE cartridge at a flow rate of 10 mL/min. The cartridge was washed again with acidified pure water to replace the last remaining inorganic ions from the SPE cartridge. After washing, the cartridge was dried under high purity grade nitrogen gas and eluted with 10 mL methanol. The extraction

efficiency ranged for all samples between 52-59% without any observed trends between the treatment trains. Limitation of this SPE method include the loss of practically all highly volatile DBPs and DOM compounds due to the drying procedure of the SPE resin prior to elution with methanol and the loss of about 40% of DOC during extraction.

Total organic carbon measurements. TOC was measured at the treatment plant and is part of a routine measurement using an Analytik Jena multi C/N 3100 analyzer with high temperature combustion.

Ultrahigh resolution mass spectrometry. Ultrahigh resolution mass spectrometry was applied to characterize the DOM and formed DBPs using a Bruker Apex QE 12 Tesla Fourier transform (FT) ion cyclotron resonance (ICR) mass spectrometer interfaced with negative ion mode electrospray ionization (ESI^-). Positive ESI (ESI^+) was not used in this study due to sodium adduct formation and much more complicated procedures to accurately assign molecular formulas, especially with the presence of high abundant isotopomers of chlorine and bromine. It is recognized here that it is likely that DBPs are missed that only ionize in ESI^+.

The spray current was set to -3.6 kV and the methanolic DOM sample was diluted with methanol at a ratio of 1:40 to obtain optimum transient spectra, which was necessary to avoid an overload of the ICR cell and the potential occurrence of peak splitting or other interferences between ions. The flow rate was set to 3 μL min^{-1} and 750 scans were acquired for each spectrum. The injection lines were washed with 600 μL (80% methanol, 20% water) between each sample to avoid cross-contamination and a carryover of samples from previous runs. Blank methanol samples were run every 5 samples and data confirmed that no carryover occurred.

This instrument achieved excellent sensitivity (mass accuracy < 0.2 ppm error after internal calibration with ubiquitous fatty acids) and yielded information about molecular ions

related to unambiguous molecular formula assignments. New custom-developed molecular formula assignment software developed at the Helmholtz Center for Environmental Health, Munich, Germany has largely automated the post processing of FT-ICR-MS data based on the following chemical elements: $^{12}C_{0-\infty}$, $^{1}H_{0-\infty}$, $^{16}O_{0-\infty}$, $^{14}N_{0-5}$ $^{32}S_{0-2,}$ $^{35}Cl_{0-3}$ and $^{79}Br_{0-3}$ isotopes, as well as the ^{13}C, ^{34}S, ^{37}Cl, and ^{81}Br isotopes. A detailed description of how to unambiguously assign molecular formulas to FT-ICR-MS data was given previously [29]. To achieve the highest degree of mass accuracy, a post calibration with known mass peaks of DOM and there exact masses and assigned molecular formulas was used throughout the observed *m/z* range (*m/z* 150-800) [30, 31]. Van Krevelen diagrams [30-37] and modified Kendrick plots [36, 38] were previously utilized to visualize FT-ICR-MS data and were also used in this study. Briefly, in a van Krevelen diagram, the elemental ratios of hydrogen to carbon (H/C) versus oxygen to carbon (O/C) of all assigned molecular formulas are plotted. This plot allows evaluating of relative hydrogen deficiency or oxygen deficiency of the assigned molecular formulas and visualizes the "chemical space" occupied by any given sample. The modified Kendrick plot is a plot, where homologous series of assigned molecular formulas, which are spaced by CH_2, can be easily depicted along the observed *m/z* range. The foundation of this modified Kendrick plot is based on the Kendrick Mass Defect (KMD) and another independent homologous series parameter referred to as z*. These parameters were previously defined and explained in detail [39].

Statistical analysis. To statistically compare in detail measured mass spectra, all *m/z* lists, including the associated intensities were combined in a single matrix, which was normalized using a logarithmic transformation to avoid single high intensity ions to unproportionally contribute to dissimilarities. Simple hierarchical cluster analyses were performed to evaluate whether or not significant differences existed between sample sets and duplicates. The Bray

Curtis similarity approach [40] with logarithmically transformed data was a robust and reliable way to show similarities between datasets and was chosen in this study.

Nuclear magnetic resonance spectroscopy. NMR spectroscopy offers quantitative depiction of compositional and structural alterations of DOM and was applied to the characterization of Råberga DOM before and after disinfection with hypochlorite. NMR spectra of solid-phase extracted DOM were acquired immediately after sample preparation with a Bruker Avance III NMR spectrometer operating at 500.13 MHz for ^{1}H with a 5 mm z-gradient dual $^{13}C/^{1}H$ cryogenic probe in $^{12}CD_3OD$ (99.8% ^{2}H; < 0.05% ^{13}C; Aldrich, Steinheim, Germany) and 3.0 mm Bruker MATCH NMR tubes. ^{1}H NMR chemical shift references were HD_2OD: 3.30 ppm and $^{12}CD_3OD$: 49.00 ppm. All spectra were acquired with TopSpin 3.2/PL3 software at 283 K and acquisition parameters matched those previously used [41] and are provided in the Supporting Information (Tab. S1).

Results and Discussion

Ultrahigh resolution mass spectra revealed detailed changes in the DOM pool during water treatments in the treatment plant (Fig. 1). Statistical evaluation using hierarchical cluster analysis revealed significant differences between the DOM in the intake, after flocculation, and after disinfection with hypochlorite (Fig. 2). A direct comparison between intake water SPE-DOM and final product water DOM showed substantial differences in the molecular composition at each nominal mass (NM), with a large contribution of newly formed chlorinated DBPs (Fig. 1).

Flocculation did change the DOM drastically, with large shifts in relative abundances across the entire pool of DOM. These changes are visualized using van Krevelen or elemental

plots before and after flocculation (Fig. 3). The presumably polyphenolic-like DOM (e.g. tannins, lignins, etc.), including CDOM, were preferentially removed by flocculation (Fig. 3), which was indicated by the removal of compounds with rather low H/C ratios (0.4-1.2) and medium to high O/C ratios (0.5-0.9). The rank correlated molecular ions that highly correlated with humic-like fluorescent peaks in a previous study [42] were similar to the ions removed by flocculation in this study and hence support the assumption that the removed molecular ions are part of the CDOM pool.

The disinfection step induced the largest changes in the molecular composition of DOM (Figs. 1, 2 and 4). Even though flocculation substantially removed DOM components, it did not prevent the formation of DBPs, presumably due to the relatively high levels of remaining TOC that were less effectively removed by flocculation. In fact, a large number (~800) of *m/z* peaks that were unambiguously assigned to molecular formulas with one, two or three chlorine atoms were formed during disinfection (Fig. 4). This is a conservative approach and only ions that showed a relative abundance of more than 0.2 % were included. In general, chlorine- or bromine-containing molecular formulas can be confirmed using isotope simulation because of the high abundance of their higher mass isotopes ^{37}Cl (37%) and ^{81}Br (49%) and respective distinctive isotope patterns. Only two brominated ions were confirmed with a threshold of 0.2 % of relative abundance. The evaluation of homologous series (molecular formulas that have a spacing of CH_2-groups) revealed the systematic formation of DBP homologous series throughout the observed mass range between 200 and 600 Da (Fig. 4).

We also discovered three highly abundant DBPs and isotopic simulation confirmed the correct molecular formula assignment and these DBPs may have been observed previously as possible drinking water related DBPs, but at much less mass resolution without the capability to

assign exact molecular formulas [43]. The molecular formulas of this specific class of DBPs (with pronounced unsaturation and absence of hydrogen) and the low carbon number implied very limited isomeric possibilities (Fig. 5). Given the constraints of FT-ICR-MS in determining exact isotope ratios, the isotope simulation matched the expected pattern of suggested molecular formulas and the only plausible structures for these compounds were either halogenated furoic acids: trichloro furoic acid, dichloro-bromo furoic acid and dibromo-chloro furoic acid or their 2,2,4-trihalo-5-hydroxy-4-cyclopentene-1,3-dione analogues (Fig. 5). The rel. abundances of trichloro, dichloro-bromo and dibromo-chloro compounds were 2.1 %, 2.26% and 0.67%, respectively. The increased abundance of the dichloro-bromo compounds when compared to trichloro compounds was at first surprising given the fact that other brominated DBPs were very low and consequently the rel. abundance should drastically decrease with increasing number of bromine atoms. However, given the fact that the ion guide frequencies cannot be optimized for any given mass ion, the low mass ions were likely to be much less efficiently transported to the ICR cell with the settings used and would mean that rel. abundances of low molecular weight ions are somewhat lower than they should be if ion guides would have been optimized for lower masses. This suggestion is supported by the rel. abundance of DOM ions in comparison to the halogenated furoic acids or 2,2,4-trihalo-5-hydroxy-4-cyclopentene-1,3-diones (trihaloHCDs) (NM: 213, 257 and 301) and the ratio of these halogenated compounds to the maximum abundant DOM ions at that NM. It can be clearly seen in Figure 5 that the peak height of the halogenated furoic acids or trihaloHCDs relative to the peak heights of DOM ions was dramatically decreasing with increasing number of bromine atoms, which was expected and which was not contradicting the low abundance of other brominated DBPs, but it nevertheless underlined the rel. high abundance of these halogenated furoic acids or trihaloHCDs. Bromide

was not measured during this study, which makes it difficult to evaluate the production of brominated DBPs.

At present, it is not clear to what extent the two abundant classes of compounds (trihalofuroic acids or trihaloHCDs) are present in our samples, but a recent study points towards trihalo HCDs [17]. These authors confirmed the structure of ion clusters similar to the ones found in this study by using MS fragmentation patterns and concluded that the molecular formulas of $C_5HO_3Cl_2Br$ and $C_5HO_3ClBr_2$ corresponded to 2,2,4-dichlorobromo-5-hydroxy-4-cyclopentene-1,3-dione and 2,2,4-dibromochloro-5-hydroxy-4-cyclopentene-1,3-dione, respectively. These trihaloHCDs appear to further react quickly with additional free chlorine to form HAAs and THMs [43], hence can be considered to be intermediate DBPs. Their reactivity is of great concern and may well play an important role in toxicological effects.

In addition to the trihaloHCDs, a large group of halogenated low molecular weight assigned formulas (less than 10 carbon atoms) were remarkably similar, and their H/C and O/C ratios suggested a polyphenol-type or aromatic acid-type structure, indicating another class of DBPs. We explored this possibility and we could find plausible, mainly hydroxyphenolic and aromatic acids for formulas with less than 10 carbon atoms (Tab. 1). Higher molecular weight molecules of assigned formulas may also represent this polyphenolic/aromatic acid class but opportunities to form isomeric structures increase rapidly with increasing weight, and hence, we chose only to give compound examples of formulas that contained less than 10 carbon atoms. Even formulas with 10 carbon atoms have already a large number of chemically reasonable isomeric structures and the given polyphenolic/aromatic acids (Tab. 1) are only intended as guidance of which type of molecules may be halogenated. However, it is chemically sound that

polyphenolic and aromatic acids are susceptible to halogenation, as has been demonstrated in previous studies [17, 43-46].

The hierarchical cluster analysis of all DOM samples throughout the treatment process, in tandem with a large chemical diversity of DBPs found, indicated a significant transformation of DOM during disinfection and supported earlier findings of a complex mixture of non-volatile DBPs [22, 23, 46] that are formed during disinfection. The majority of these DBPs are likely the product of the reaction of HOCl with aromatic polyphenolic-type compounds. Earlier research has shown that humic and fulvic acids, which constitute a large component of the DOM in natural waters, are composed of polyphenolic structures [47]. We could not confirm brominated DBPs beside the above mentioned trihaloHCDs, and this is likely due to a very low abundance of brominated DBPs. A few potential brominated compounds were found, but they did not exceed 0.2 % relative abundance and isotope simulation was not conclusive at their low abundance.

Overall, ^{1}H and ^{13}C NMR spectra looked rather unchanged before and after chlorination, suggesting minor overall alterations of DOM chemistry (Supporting Information: Tabs. S1 and S2). This is consistent with bulk total organic halogen (TOX) measurements (representing total chloro-, bromo-, and iodo-DBPs) observed for chlorinated water, in which only a low percentage of TOX is formed compared to the initial non-halogenated DOM. For example, in the U.S. Nationwide Occurrence Study, a median level of 178 $\mu g\ L^{-1}$ levels of TOX was formed from a median level of 5.8 $mg\ L^{-1}$ (5800 $\mu g\ L^{-1}$) of TOC with the use of chorine and other disinfectants [18].

Difference ^{1}H NMR spectroscopy and NMR spectral editing did reveal a molecular variance of DOM as a consequence of chlorination (Fig. 6). New, weak but rather sharp NMR resonances appeared in DOM following chlorination, testifying to the presence of distinct

molecules which were formed during chlorination. Overall, the NMR integral of ^{1}H NMR resonances ranged below 2%, implying that the bulk DOM characteristics still dominated over newly formed molecules (similar to earlier TOX measurements mentioned above [48]). Chlorination led to a relative increase of functionalized aliphatic units (i. e. **H**CCX units; δ_H: 1.8 - 2.9 ppm) and a marked AA´B-multiplet structure (δ_H = 3.510 ppm: 2H, dd, J = 11.2, 6.0 Hz; δ_H = 3.582 ppm; 2H, dd, J = 11.2, 4.8 Hz; δ_H = 3.652 ppm: 1H, pentett, J = 5.5 Hz). The abundance of compounds resonating in the section of esters and other highly oxygenated aliphatic compounds also increased in abundance (δ_H > 4). However, this section of the difference NMR spectrum may also represent newly formed chlorinated aliphatic compounds and might also become affected from differential solvent suppression in both DOM samples. Nevertheless, tiny newly formed NMR resonances remained visible. Olefins (δ_H: 5.15 – 6.1 ppm) as well as some neutral and oxygenated aromatics or halogenated aromatics (δ_H > 7.05 ppm) increased in abundance after chlorination. In contrast, pure aliphatic compounds (i.e. **H**C_nC units; n > 2; δ_H < 1.9 ppm), methoxy groups in various chemical environments as well as possibly carbohydrates (OC**H**, OC**H**$_3$, δ_H: 3.65 - 4 ppm) and α,β-unsaturated olefins and phenolic compounds (δ_H: 6.1 – 7.05 ppm) decreased in abundance during chlorination. The decrease in OC**H** of phenols is consistent with an increase in chlorinated phenols as suggested by the FT-MS data. Chlorination of unsaturated bonds (=CH) and the formation of =C-Cl moieties which resonate in this section of proton NMR chemical shift was likely to interfere with this basic interpretation. Alternatively, aliphatic **H**CCl_2-units will resonate near δ_H = 5.6 ppm; i.e. in the nominal ^{1}H NMR chemical shift section of O_2C**H** and =C**H** groups. The addition of a chlorine atom to organic molecules causes in general a rather large shift (~3 δ_H) and is likely to be responsible for the apparent

increase in hydrogens associated with aromatic (H_{ar}) and hydrogens in other unsaturated compounds (**H**C=C) (Tab. S1) and complicating the analysis of ^{1}H NMR section integrals.

Difference NMR spectra of single pulse ^{13}C NMR spectra showed an insufficient S/N ratio for allowing unambiguous conclusions about structural alterations initiated by chlorination. However, the abundance of methoxy groups declined visibly (Supporting Information: Fig. S2 and Tab. S3). Further research is needed to more precisely determine the precursors of DBP formation, and it can be envisioned that bulk parameters, such as measurements of total phenolic content [49] may help to predict DBP formation.

By using new advanced technologies, such as ultrahigh resolution non-target analyses, this study revealed a large number of new and potentially important DBPs. Our study illustrates that humans may be exposed to a complex mixture of DBPs of unknown structure and toxicity. The large number of halogenated ions found in this study and the much larger number of unknown but potentially synergistic biological effects pose an important human health challenge in preventing DBP formation while guarantee efficient disinfection.

Non-target ultrahigh resolution techniques have demonstrated the importance to reveal the magnitude of DBP formation and a possible next step forward is to further constrain the classes of DBPs that are formed and link these with DOM precursors. One way to achieve further separation and information of polarity-based classes of DBP compounds is the implementation of liquid chromatography-based separation prior to ultrahigh resolution mass spectrometry. Modern ultrahigh pressure liquid chromatography (UPLC) and complementary stationary phases (e.g. reversed phase versus amino based) could drastically constrain classes of newly discovered DBPs, prior to FT-MS analysis.

Acknowledgements

The advanced analytical instrumentation located at the Helmholtz Center for Environmental Health in Munich, Germany, enabled critical non-target organic structural spectroscopy. This study was financially supported by the Swedish Research Council FORMAS (Grant 2013-1077). We also thank Tekniska Verken, Linköping for cooperation and data sharing. This is contribution XXXX from the University of Maryland Center for Environmental Science, Chesapeake Biological Laboratory.

Supporting Information Available

The supporting information includes tables and details about ^{1}H and ^{13}C-NMR cross section integrals of DOM before and after disinfection (Tab. S1 and S2), a figure about TOC concentrations measured betwee 2011-2013 (Fig. S1), as well as the ^{13}C-NMR spectra before and after disinfection (Fig. S2). These are the tables and figures referred to in the main text. The supporting information is available free of charge via the Internet at http://pubs.acs.org/

References

1. Rook, J. J., Formation of haloforms during chlorination of natural waters. *Water Treatment Examination* **1974**, (23), 234-243.
2. National Cancer Institute *Report On Carcinogenesis Bioassay of Chloroform (CAS No. 67-66-3)*; National Cancer Institute: Bethesda, MD, 1976.
3. Bull, R. J.; Reckhow, D. A.; Li, X.; Humpage, A. R.; Joll, C.; Hrudey, S. E., Potential carcinogenic hazards of non-regulated disinfection by-products: haloquinones, halo-cyclopentene and cyclohexene derivatives, N-halamines, halonitriles, and heterocyclic amines. *Toxicology* **2011,** *286*, (1-3), 1-19.
4. Costet, N.; Garlantezec, R.; Monfort, C.; Rouget, F.; Gagniere, B.; Chevrier, C.; Cordier, S., Environmental and Urinary Markers of Prenatal Exposure to Drinking Water Disinfection By-Products, Fetal Growth, and Duration of Gestation in the PELAGIE Birth Cohort (Brittany, France, 2002-2006). *American Journal of Epidemiology* **2012,** *175*, (4), 263-275.
5. Ding, G.; Zhang, X., A Picture of Polar Iodinated Disinfection Byproducts in Drinking Water by (UPLC/)ESI-tqMS. *Environ. Sci. Technol.* **2009,** *43*, (24), 9287-9293.
6. Grazuleviciene, R.; Nieuwenhuijsen, M. J.; Vencloviene, J.; Kostopoulou-Karadanelli, M.; Krasner, S. W.; Danileviciute, A.; Balcius, G.; Kapustinskiene, V., Individual exposures to drinking water trihalomethanes, low birth weight and small for gestational age risk: a prospective Kaunas cohort study. *Environmental Health* **2011,** *10*.
7. Nieuwenhuijsen, M. J.; Toledano, M. B.; Eaton, N. E.; Fawell, J.; Elliott, P., Chlorination disinfection byproducts in water and their association with adverse reproductive outcomes: a review. *Occupational and Environmental Medicine* **2000,** *57*, (2), 73-85.
8. Richardson, S. D.; Ternes, T. A., Water Analysis: Emerging Contaminants and Current Issues. *Analytical chemistry* **2014,** *86*, (6), 2813-2848.
9. Richardson, S. D., Disinfection By-Products: Formation and Occurrence in Drinking Water. In *Encyclopedia of Environmental Health*, Nriagu, J., Ed. Elsevier Science: Burlington, 2011; pp 110-136.
10. Richardson, S. D.; Nriagu, J. O., *The Encyclopedia of Environmental Health*. 2011; Vol. 2, p 110.
11. Richardson, S. D.; Plewa, M. J.; Wagner, E. D.; Schoeny, R.; DeMarini, D. M., Occurrence, genotoxicity, and carcinogenicity of regulated and emerging disinfection by-products in drinking water: A review and roadmap for research. *Mutation Research-Reviews in Mutation Research* **2007,** *636*, (1-3), 178-242.
12. Savitz, D. A.; Singer, P. C.; Herring, A. H.; Hartmann, K. E.; Weinberg, H. S.; Makarushka, C., Exposure to drinking water disinfection by-products and pregnancy loss. *American Journal of Epidemiology* **2006,** *164*, (11), 1043-1051.
13. Villanueva, C. M.; Gracia-Lavedan, E.; Ibarluzea, J.; Santa Marina, L.; Ballester, F.; Llop, S.; Tardon, A.; Fernandez, M. F.; Freire, C.; Goni, F.; Basagana, X.; Kogevinas, M.; Grimalt, J. O.; Sunyer, J.; Infancia, I.; Medio, A., Exposure to Trihalomethanes through Different Water Uses and Birth Weight, Small for Gestational Age, and Preterm Delivery in Spain. *Environmental Health Perspectives* **2011,** *119*, (12), 1824-1830.
14. Villanueva, C. M.; Cantor, K. P.; Cordier, S.; Jaakkola, J. J. K.; King, W. D.; Lynch, C. F.; Porru, S.; Kogevinas, M., Disinfection byproducts and bladder cancer - A pooled analysis. *Epidemiology* **2004,** *15*, (3), 357-367.

15. Waller, K.; Swan, S. H.; DeLorenze, G.; Hopkins, B., Trihalomethanes in drinking water and spontaneous abortion. *Epidemiology* **1998,** *9*, (2), 134-140.
16. Waller, K.; Swan, S. H.; Windham, S. C.; Fenster, L., Influence of exposure assessment methods on risk estimates in an epidemiologic study of total trihalomethane exposure and spontaneous abortion. *Journal of Exposure Analysis and Environmental Epidemiology* **2001,** *11*, (6), 522-531.
17. Zhai, H.; Zhang, X.; Zhu, X.; Liu, J.; Ji, M., Formation of Brominated Disinfection Byproducts during Chloramination of Drinking Water: New Polar Species and Overall Kinetics. *Environ. Sci. Technol.* **2014,** *48*, (5), 2579-2588.
18. Krasner, S. W.; Weinberg, H. S.; Richardson, S. D.; Pastor, S. J.; Chinn, R.; Sclimenti, M. J.; Onstad, G. D.; Thruston, A. D., Occurrence of a New Generation of Disinfection Byproducts†. *Environ. Sci. Technol.* **2006,** *40*, (23), 7175-7185.
19. Khiari, D.; Krasner, S. W.; Hwang, C. J.; Chinn, R.; Barrett, S. In *Effects of Chlorination and Chloramination on the Molecular Weight Distribution of Natural Organic Matter and the Production of High-Molecular-Weight Disinfection By-Products*, AWWA Water Technology Conference, Boston, MA, 1996; American Water Works Association: Boston, MA, 1996.
20. Zhang, X.; Minear, R. A., Characterization of High Molecular Weight Disinfection Byproducts Resulting from Chlorination of Aquatic Humic Substances. *Environmental Science & Technology* **2002,** *36*, (19), 4033-4038.
21. Zhang, X.; Minear, R. A., Formation, adsorption and separation of high molecular weight disinfection byproducts resulting from chlorination of aquatic humic substances. *Water Research* **2006,** *40*, (2), 221-230.
22. Lavonen, E. E.; Gonsior, M.; Tranvik, L. J.; Schmitt-Kopplin, P.; Köhler, S. J., Selective Chlorination of Natural Organic Matter: Identification of Previously Unknown Disinfection Byproducts. *Environ. Sci. Technol.* **2013,** *47*, (5), 2264-2271.
23. Zhang, H.; Zhang, Y.; Shi, Q.; Hu, J.; Chu, M.; Yu, J.; Yang, M., Study on Transformation of Natural Organic Matter in Source Water during Chlorination and Its Chlorinated Products using Ultrahigh Resolution Mass Spectrometry. *Environ. Sci. Technol.* **2012,** *46*, (8), 4396-4402.
24. Zhang, X.; Minear, R. A.; Barrett, S. E., Characterization of High Molecular Weight Disinfection Byproducts from Chlorination of Humic Substances with/without Coagulation Pretreatment Using UF−SEC−ESI-MS/MS. *Environmental Science & Technology* **2005,** *39*, (4), 963-972.
25. U.S. Environmental Protection Agency, National Primary Drinking Water Regulations: Stage 2 Disinfectants and Disinfection Byproducts Rule. In Federal Register: 2006; Vol. 71, p 388.
26. The Council of the European Union, COUNCIL DIRECTIVE 98/83/EC of 3 November 1998 on the quality of water intended for human consumption. In Official Journal of the European Communities: 1998; p L 330/32.
27. Dittmar, T.; Koch, B.; Hertkorn, N.; Kattner, G., A simple and efficient method for the solid-phase extraction of dissolved organic matter (SPE-DOM) from seawater. *Limnol. Oceanogr.: Methods* **2008,** *6*, (June), 230-235.
28. Boutegrabet, L.; Kanawati , B.; Gebefügi, I.; Peyron, D.; Cayot, P.; Gougeon, R. D.; Schmitt-Kopplin , P., Attachment of Chloride Anion to Sugars: Mechanistic Investigation and Discovery of a New Dopant for Efficient Sugar Ionization/Detection in Mass Spectrometers. *Chemistry – A European Journal* **2012,** *18*, (41), 13059-13067.

29. Koch, B. P.; Dittmar, T.; Witt, M.; Kattner, G., Fundamentals of molecular formula assignment to ultrahigh resolution mass data of natural organic matter. *Analytical chemistry* **2007,** *79*, (4), 1758-63.
30. Gonsior, M.; Peake, B. M.; Cooper, W. T.; Podgorski, D.; D'Andrilli, J.; Cooper, W. J., Photochemically Induced Changes in Dissolved Organic Matter Identified by Ultrahigh Resolution Fourier Transform Ion Cyclotron Resonance Mass Spectrometry. *Environ. Sci. Technol.* **2009,** *43*, 698-703.
31. Gonsior, M.; Peake, B. M.; Cooper, W. T.; Podgorski, D. C.; D'Andrilli, J.; Dittmar, T.; Cooper, W. J., Characterization of dissolved organic matter across the Subtropical Convergence off the South Island, New Zealand. *Marine Chemistry* **2011,** *123*, (1-4), 99-110.
32. Kim, S.; Kramer, R. W.; Hatcher, P. G., Graphical Method for Analysis of Ultrahigh-Resolution Broadband Mass Spectra of Natural Organic Matter, the Van Krevelen Diagram. *Anal. Chem.* **2003,** *75*, (20), 5336-5344.
33. Hertkorn, N.; Frommberger, M.; Witt, M.; Koch, B.; Schmitt-Kopplin, P.; Perdue, E. M., Natural Organic Matter and the Event Horizon of Mass Spectrometry. *Analytical Chemistry* **2008,** *80*, (23), 8908-8919.
34. Dittmar, T., The molecular level determination of black carbon in marine dissolved organic matter. *Org. Geochem.* **2008,** *39*, (Copyright (C) 2011 American Chemical Society (ACS). All Rights Reserved.), 396-407.
35. Flerus, R.; Lechtenfeld, O. J.; Koch, B. P.; McCallister, S. L.; Schmitt-Kopplin, P.; Benner, R.; Kaiser, K.; Kattner, G., A molecular perspective on the ageing of marine dissolved organic matter. *Biogeosciences* **2012,** *9*, (6), 1935-1955.
36. Gonsior, M.; Schmitt-Kopplin, P.; Bastviken, D., Depth-dependent molecular composition and photo-reactivity of dissolved organic matter in a boreal lake under winter and summer conditions. *Biogeosciences* **2013,** *10*, (11), 6945-6956.
37. Sleighter, R. L.; Hatcher, P. G., Molecular characterization of dissolved organic matter (DOM) along a river to ocean transect of the lower Chesapeake Bay by ultrahigh resolution electrospray ionization Fourier transform ion cyclotron resonance mass spectrometry. *Mar. Chem.* **2008,** *110*, (3-4), 140-152.
38. Shakeri Yekta, S.; Gonsior, M.; Schmitt-Kopplin, P.; Svensson, B. H., Characterization of Dissolved Organic Matter in Full Scale Continuous Stirred Tank Biogas Reactors Using Ultrahigh Resolution Mass Spectrometry: A Qualitative Overview. *Environ. Sci. Technol.* **2012,** *46*, (22), 12711-12719.
39. Stenson, A. C.; Marshall, A. G.; Cooper, W. T., Exact Masses and Chemical Formulas of Individual Suwannee River Fulvic Acids from Ultrahigh Resolution Electrospray Ionization Fourier Transform Ion Cyclotron Resonance Mass Spectra. *Anal. Chem.* **2003,** *75*, (6), 1275-1284.
40. Bray, J. R.; Curtis, J. T., An Ordination of the Upland Forest Communities of Southern Wisconsin. *Ecological Monographs* **1957,** *27*, (4), 325-349.
41. Gonsior, M.; Hertkorn, N.; Conte, M. H.; Cooper, W. J.; Bastviken, D.; Druffel, E.; Schmitt-Kopplin, P., Photochemical production of polyols arising from significant photo-transformation of dissolved organic matter in the oligotrophic surface ocean. *Marine Chemistry* **2014,** *163*, (0), 10-18.
42. Herzsprung, P.; von Tümpling, W.; Hertkorn, N.; Harir, M.; Büttner, O.; Bravidor, J.; Friese, K.; Schmitt-Kopplin, P., Variations of DOM Quality in Inflows of a Drinking Water

Reservoir: Linking of van Krevelen Diagrams with EEMF Spectra by Rank Correlation. *Environ. Sci. Technol.* **2012,** *46*, (10), 5511-5518.
43. Zhai, H.; Zhang, X., Formation and Decomposition of New and Unknown Polar Brominated Disinfection Byproducts during Chlorination. *Environ. Sci. Technol.* **2011,** *45*, (6), 2194-2201.
44. Gallard, H.; von Gunten, U., Chlorination of Phenols: Kinetics and Formation of Chloroform. *Environ. Sci. Technol.* **2002,** *36*, (5), 884-890.
45. Rebenne, L. M.; Gonzalez, A. C.; Olson, T. M., Aqueous Chlorination Kinetics and Mechanism of Substituted Dihydroxybenzenes. *Environ. Sci. Technol.* **1996,** *30*, (7), 2235-2242.
46. Pan, Y.; Zhang, X., Four Groups of New Aromatic Halogenated Disinfection Byproducts: Effect of Bromide Concentration on Their Formation and Speciation in Chlorinated Drinking Water. *Environ. Sci. Technol.* **2013,** *47*, (3), 1265-1273.
47. Thurman, E. M., *Organic Geochemistry of Natural Waters*. Martinus Nijhoff/Dr. W. Junk Publishers: Dordrecht, 1985; Vol. 2.
48. Chai, W.-M.; Liu, X.; Hu, Y.-H.; Feng, H.-L.; Jia, Y.-L.; Guo, Y.-J.; Zhou, H.-T.; Chen, Q.-X., Antityrosinase and antimicrobial activities of furfuryl alcohol, furfural and furoic acid. *International Journal of Biological Macromolecules* **2013,** *57*, (0), 151-155.
49. Takeda, K.; Moriki, M.; Oshiro, W.; Sakugawa, H., Determination of phenolic concentrations in dissolved organic matter pre-concentrate using solid phase extraction from natural water. *Marine Chemistry* **2013,** *157*, 208-215.

Table 1: FT-MS results of the most intense DBP-related ions, as well as DBP ions that contain 10 or less carbon atoms and have a mass lower than 240 Da. Theoretical examples of polyphenolic and aromatic acids that match the assigned molecular formulas are also shown. Note: All formulas were confirmed by isotopic simulation and the presence of the ^{37}Cl, and if applicable, the ^{81}Br isotope.

Most abundant DBPs	**Mass measured $(M-H)^-$**	**Intensity (TIC)**	**Exact Mass (neutral)**	**Molecular Formula (M)**	**KMD**	**O/C**	**H/C**	**DBE**	**DBE/C**
2,2,4-trichloro-5-hydroxy-4-cyclopentene-1,3-dione	212.89195	73570248	213.89913	C5HO3Cl3	0.340	0.600	0.200	4	0.800
2,2,4-dichlorobromo-5-hydroxy-4-cyclopentene-1,3-dione	256.84130	79120600	257.84861	C5HO3Cl2Br	0.439	0.600	0.200	4	0.800
2,2,4-chlorodibromo-5-hydroxy-4-cyclopentene-1,3-dione	300.79090	23593458	301.79810	C5HO3ClBr2	0.539	0.600	0.200	4	0.800
Possible chlorinated polyphenolic and aromatic acids									
chlorophthalic acid	198.98044	5253117	199.98763	C8H5O4Cl1	0.236	0.500	0.625	6	0.750
chlorophloretic acid	199.01677	5412670	200.02402	C9H9O3Cl1	0.199	0.333	1.000	5	0.556
chloro-orsellinic acid	200.99595	8649003	202.00329	C8H7O4Cl1	0.222	0.500	0.875	5	0.625
dichloro-orsellinic acid	234.95704	10247170	235.96432	C8H6O4Cl2	0.299	0.500	0.750	5	0.625
chlorogallic acid	202.97535	6198405	203.98255	C7H5O5Cl1	0.245	0.714	0.714	5	0.714
dichlorogallic acid	236.93641	7044813	237.94358	C7H4O5Cl2	0.322	0.714	0.571	5	0.714
chloromethoxyphenylacrylic acid	211.01672	5943678	212.02402	C10H9O3Cl1	0.213	0.300	0.900	6	0.600
chlorodihydroxycinnamic acid	212.99611	11082396	214.00329	C9H7O4Cl1	0.236	0.444	0.778	6	0.667
chloromethoxyhydrocinnamic acid	213.03239	6392293	214.03967	C10H11O3Cl1	0.199	0.300	1.100	5	0.500
chlorohydroxyphthalic acid	214.97521	11232844	215.98255	C8H5O5Cl1	0.259	0.625	0.625	6	0.750
chlorodimethoxybenzoic acid	215.01169	12298902	216.01899	C9H9O4Cl1	0.222	0.444	1.000	5	0.556
chlorodihydroxymandelic acid	216.99100	10869836	217.99820	C8H7O5Cl1	0.245	0.625	0.875	5	0.625
dichlorohydroxyphenylacetic acid	218.96214	5940199	219.96940	C8H6O3Cl2	0.276	0.375	0.750	5	0.625
dichlorodihydroxybenzoic acid	220.94148	10401146	221.94867	C7H4O4Cl2	0.299	0.571	0.571	5	0.714
chlorodihydroxy-naphthoquinone	222.98040	10615130	223.98764	C10H5O4Cl1	0.262	0.400	0.500	8	0.800
chloroscopoletin	224.99606	9621716	226.00329	C10H7O4Cl1	0.249	0.400	0.700	7	0.700
chlorocarboxycarbonylbenzoic acid	226.97526	13598656	227.98255	C9H5O5Cl1	0.272	0.556	0.556	7	0.778
chloroferulic acid	227.01175	14956549	228.01894	C10H9O4Cl1	0.236	0.400	0.900	6	0.600
chloromethoxyphthalic acid	228.99103	16821404	229.99820	C9H7O5Cl1	0.259	0.556	0.778	6	0.667
chlorosyringic acid	231.00666	19996432	232.01385	C9H9O5Cl1	0.245	0.556	1.000	5	0.556

chlorotrihydroxy-methoxybenzoic acid	232.98589	6958285	233.99312	C8H7O6Cl1	0.268	0.750	0.875	5	0.625

Note: TIC = Total Ion Count; KMD = Kendrick Mass Defect; O/C = oxygen to carbon ratio; H/C = hydrogen to carbon ratio; DBE = Double Bond Equivalency; DBE/C = Double Bond Equivalency divided by carbon number

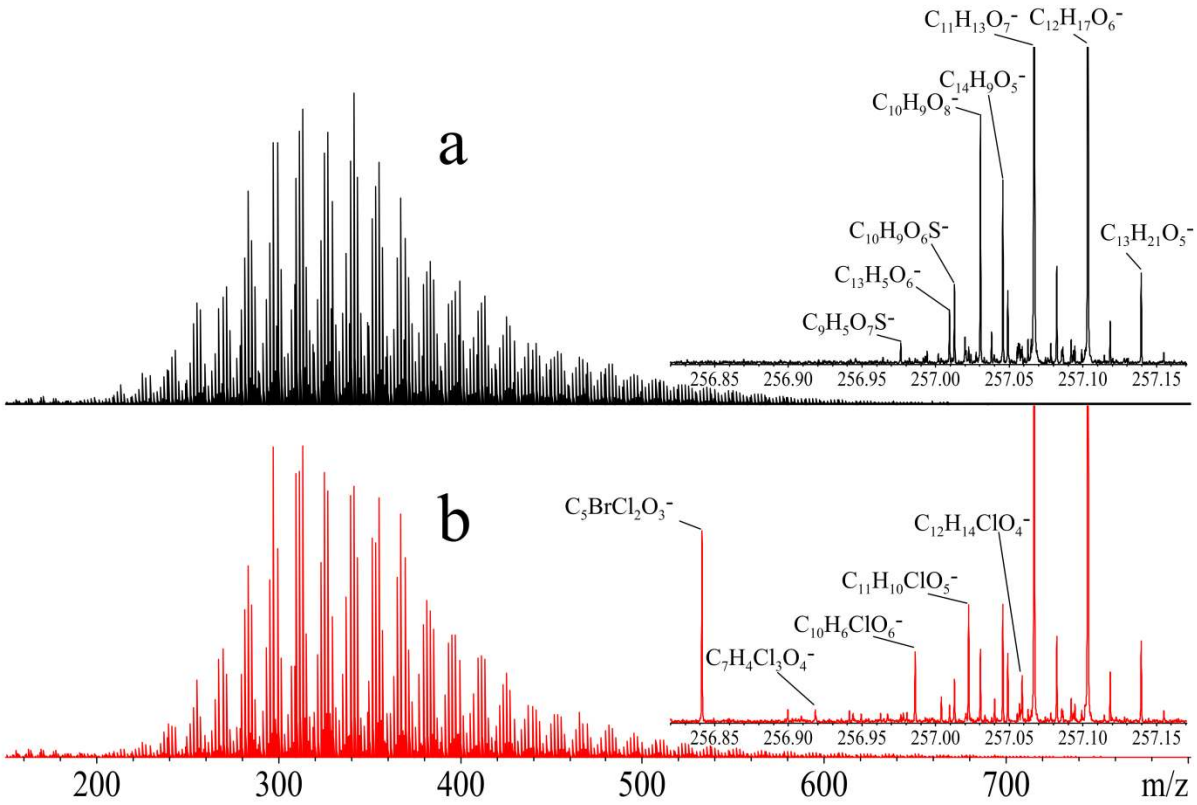

Figure 1: Ultrahigh resolution mass spectra of raw water DOM (a) and after disinfection (b), including the molecular formula assignments of major ions at NM 257.

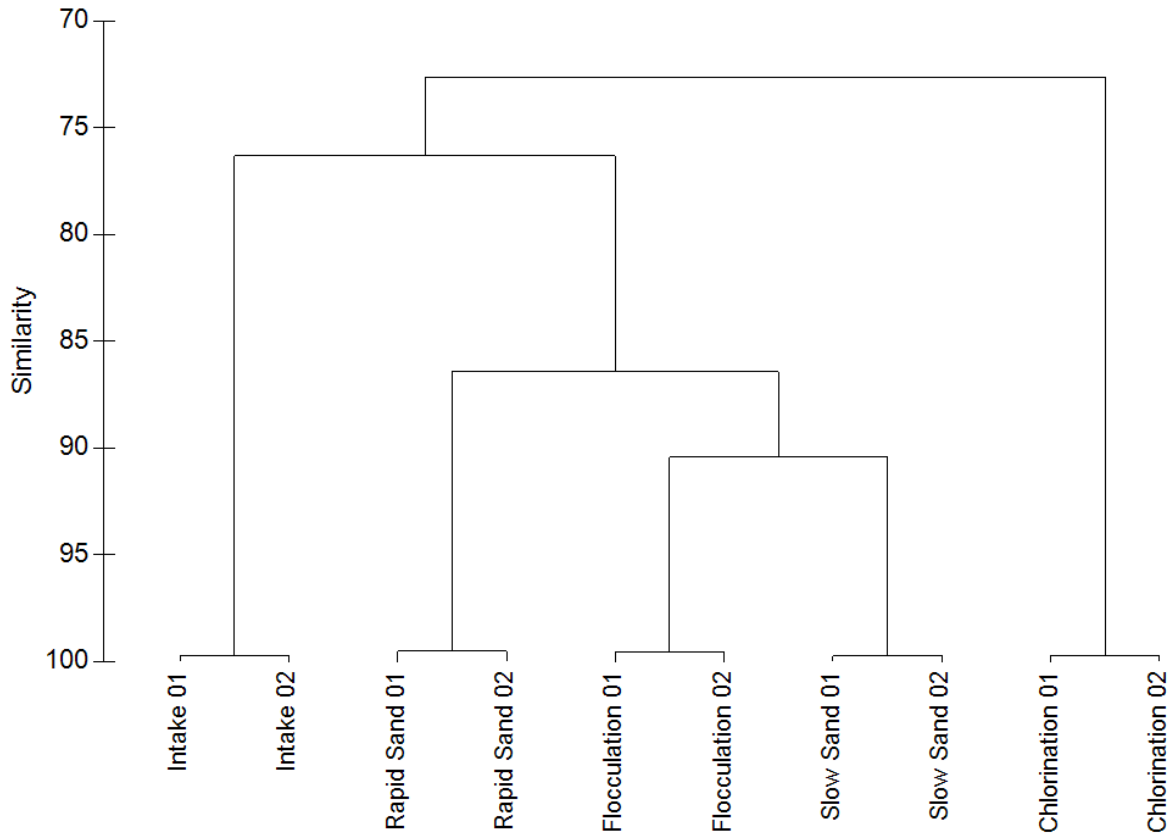

Figure 2: Hierarchical cluster analysis of duplicate sampling throughout the different water treatments. Note: The FT-ICR-MS data was logarithmically transformed prior to Bray Curtis Similarity resemblance calculations.

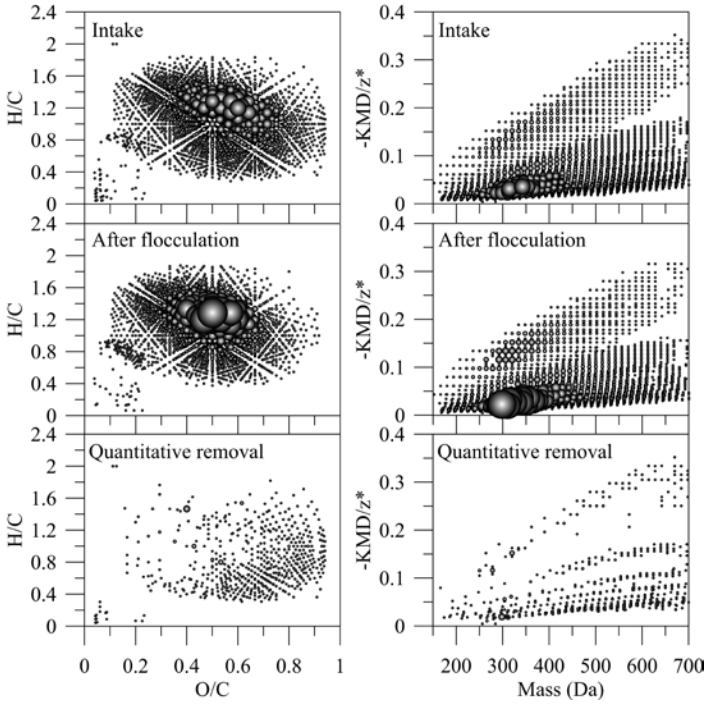

Figure 3: Van Krevelen diagrams and modified Kendrick plots (-KMD/z* versus mass) of the DOM of the raw water (intake), after flocculation and the removal of many polyphenolic-type ions and associated molecular formulas during the flocculation treatment. Note: The modified Kendrick plot (-KMD/z* versus mass) was previously described in detail [38]. The bubble areas represent the relative abundance of ions.

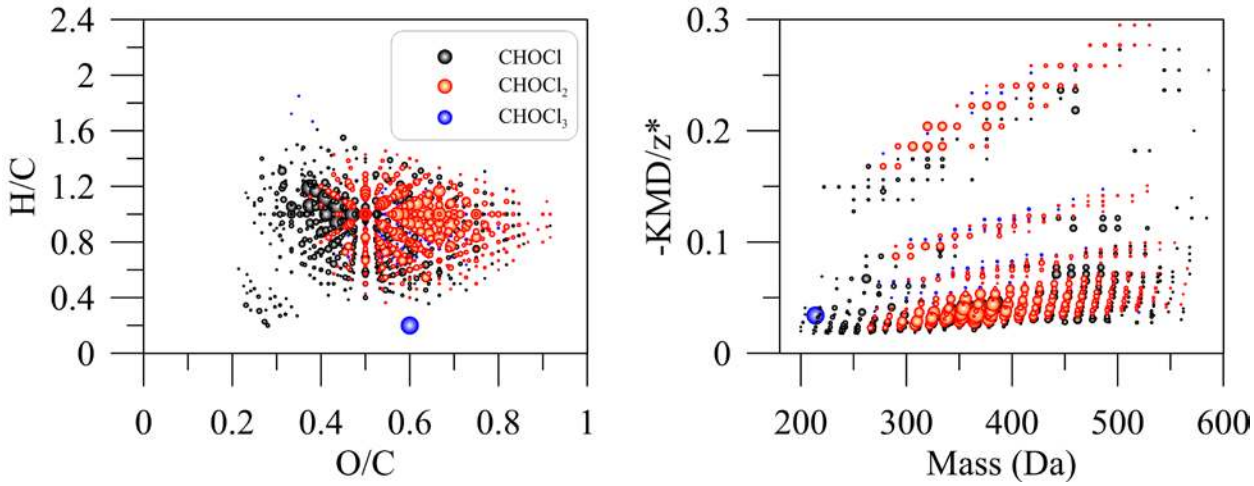

Figure 4: Production of DBPs during the disinfection by using hypochlorite and visualized using a van Krevelen and modified Kendrick plot. The bubble areas represent the relative abundance of ions.

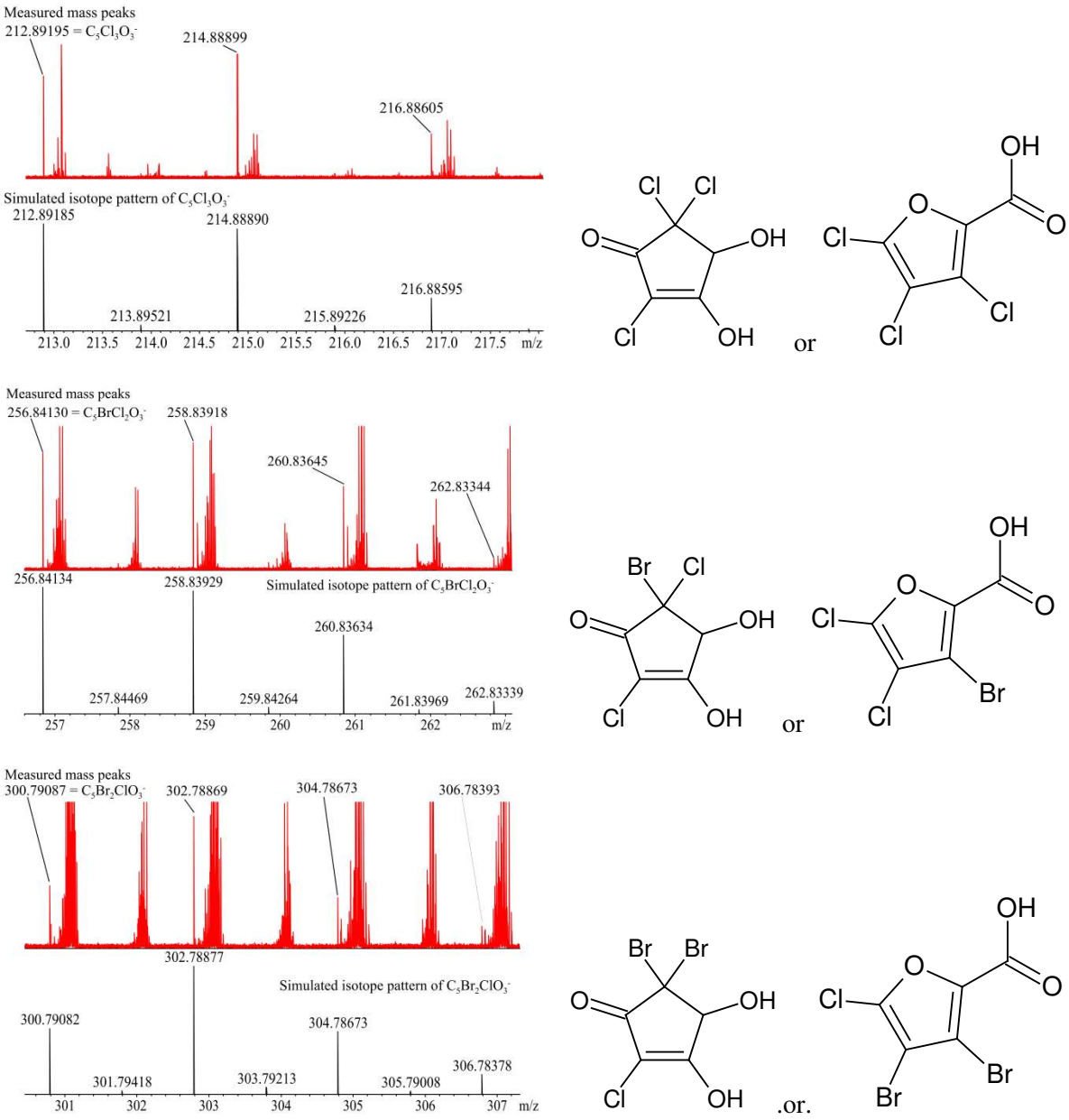

Figure 5: Some relatively high abundant ions with a large mass defect indicated the presence of halogenated compounds. The molecular formulas of these ions were confirmed by isotopic simulation and only two isomers are likely being either 2,2,4-trihalo-5-hydroxy-4-cyclopentene-1,3-diones or trihalofuroic acids.

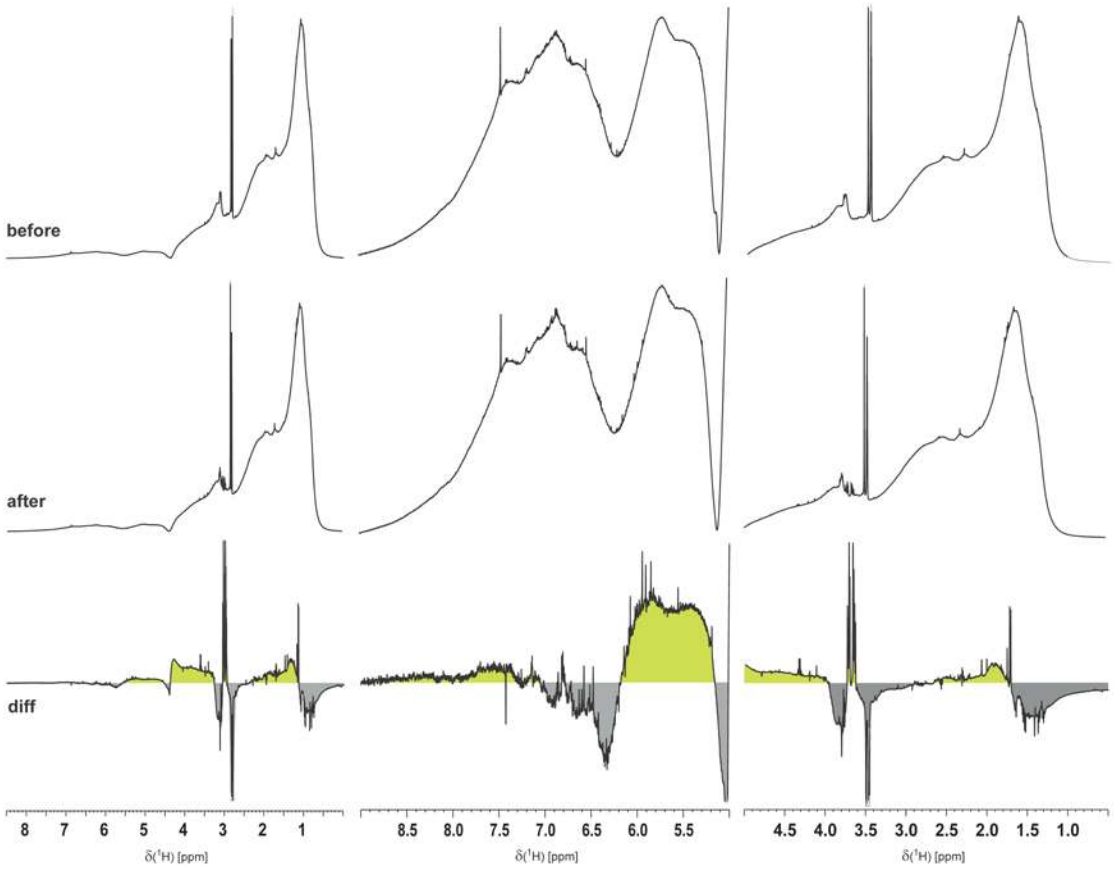

Figure 6: 1H NMR spectra of DOM (12CD3OD solution, 500 MHz) before (top) and after (middle) chlorination; bottom row: difference NMR spectrum with green: DOM features increased in relative abundance after chlorination, and gray: DOM features decreased in relative abundance after chlorination.

Supplementary Information

Changes in Dissolved Organic Matter during the Treatment Processes of a Drinking Water Plant in Sweden and Formation of Previously Unknown Disinfection Byproducts

Michael Gonsior [a*], *Philippe Schmitt-Kopplin* [b,c], *Helena Stavklint* [d], *Susan D. Richardson* [e], *Norbert Hertkorn* [b] *and David Bastviken* [f]

[a] Chesapeake Biological Laboratory , University of Maryland Center for Environmental Science, Solomons, USA

[b] Helmholtz Zentrum München, Analytical BioGeoChemistry, Neuherberg, Germany

[c] Technische Universität München, Analytical Food Chemistry, D-85354 Freising-Weihenstephan, Germany

[d] Tekniska verken i Linköping AB, Sweden

[e] University of South Carolina, Department of Chemistry and Biochemistry, Columbia, SC, USA

[f] Linköping University, Department of Thematic Studies – Environmental Change, Linköping, Sweden

[*]Corresponding author. phone: +14103267245, fax: +14103267302, Email address: gonsior@umces.edu

Summary

spectrum	Figure	NS	AQ [s]	D1 [s]	WDW2	PR2
^{1}H NMR before / after Cl	6	512	5	5	EM	1
^{13}C NMR before / after Cl	S2	9361 / 9456	1	19	EM	35 (2)
DEPT 45/135 ^{13}C NMR before / after Cl	S2	16384	1	2	EM	12.5
DEPT 90 ^{13}C NMR before / after Cl	S2	32768	1	2	EM	12.5

Table S1: Acquisition parameters of NMR spectra, shown according to figures. NS: number of scans (for 2D NMR: F2); AQ: acquisition time [ms]; D1: relaxation delay [ms]; NE: number of F1 increments in 2D NMR spectra; WDW1, WDW2: apodization functions in F1/ F2 (EM: line broadening factor [Hz]; PR2: coefficients used for windowing functions WDW2.

δ(^{1}H) [ppm]	**10 - 7.0**	**7.0 - 5.3**	**4.9 - 3.1**	**3.1 - 1.9**	**1.9 - 0.0**	$H_{olefinic}$ / $H_{aromatic}$	**10 - 5.3** (**H**C_{sp^2})
key substructures	**H**$_{ar}$	**H**C=C, **H**CO_2	**H**CO	**H**C-N, **H**C-C-X	**H**C-C-C-		
before Cl	2.4	2.1	19.2	28.7	47.6	0.9	4.5
after Cl	3.0	2.7	19.3	29.1	46.0	0.9	5.7

Table S2: ^{1}H NMR section integrals (percent of non-exchangeable protons) and key substructures of DOM before and after chlorination.

δ(^{13}C) ppm	220-187	187-167	167-145	145-108	108-90	90-47	47-0	H/C ratio	O/C ratio
Key substructures	**C**=O	**C**OX	$\underline{C}_{ar}$-O	$\underline{C}_{ar}$-C,H	$O_2\underline{C}H$	O**C**H	C**C**H		
before chlorination	1.8	9.8	3.9	8.4	5.6	33.7	36.8	**1.31**	**0.70**
after chlorination	1.7	9.1	3.8	10.8	5.6	32.1	35.5	**1.28**	**0.67**
NMR mixing model	**C=O**	**COOH**	**C_{ar}-O**	**C_{ar}-H**	**O_2CH**	**OCH**	**CH_2**		
H/C ratio	**0**	**1**	**0**	**1**	**1**	**1**	**2**		
O/C ratio	**1**	**2**	**1**	**0**	**2**	**1**	**0**		

DOM (depth)	CH total	CH_2 total	CH_3 total	ratio (d_1 / c_1 / b_1 / a_1) $H\underline{C}_{ar}$-C / O-H**C**-O / H**C**-O / H**C**-C	ratio (b_2 / a_2) $H_2\underline{C}$-O / $H_2\underline{C}$-C	ratio (b_3 / a_3) $H_3\underline{C}$-O / $H_3\underline{C}$-C
before chlorination	36	30	34	15.9 / 1.0 / 33.9 / 49.1	6.8 / 93.2	9.1 / 90.9
after chlorination	35	33	32	14.8 / 1.4 / 34.5 / 49.3	10.7 / 89.3	5.7 / 94.3*

Table S3. (Top): ^{13}C NMR section integrals (percent of total carbon) and key substructures of DOM before and after chlorination. Middle: Substructures used for NMR-derived reverse mixing model with nominal H/C and O/C ratios given. Bottom: percentage of methin, methylene and methyl carbon related to total protonated ^{13}C NMR integral as derived from ^{13}C DEPT NMR spectra of DOM according to carbon multiplicity (left 3 columns) and relative proportions of these CH_n units binding to oxygen versus carbon chemical environments.

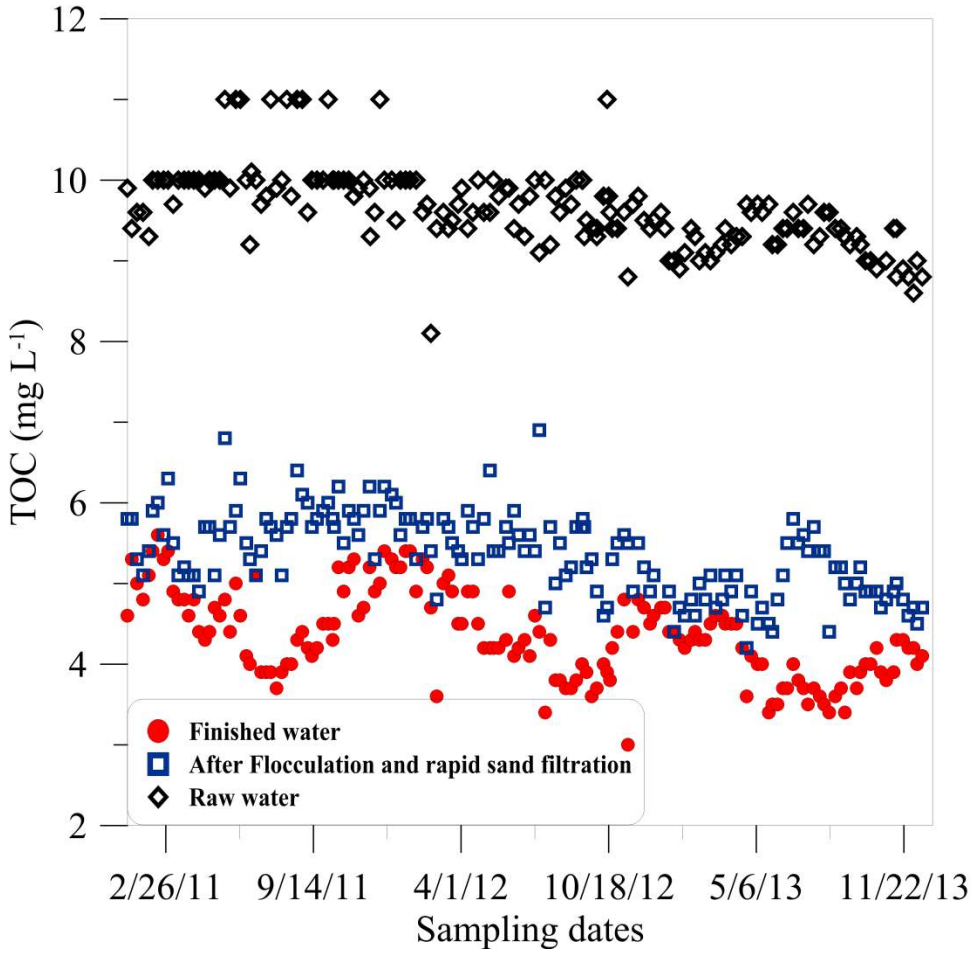

Figure S1: Total organic carbon concentration of the raw water, after flocculation/rapid sand filtration, and of the processed water, Råberga drinking water treatment plant, Linköping, Sweden.

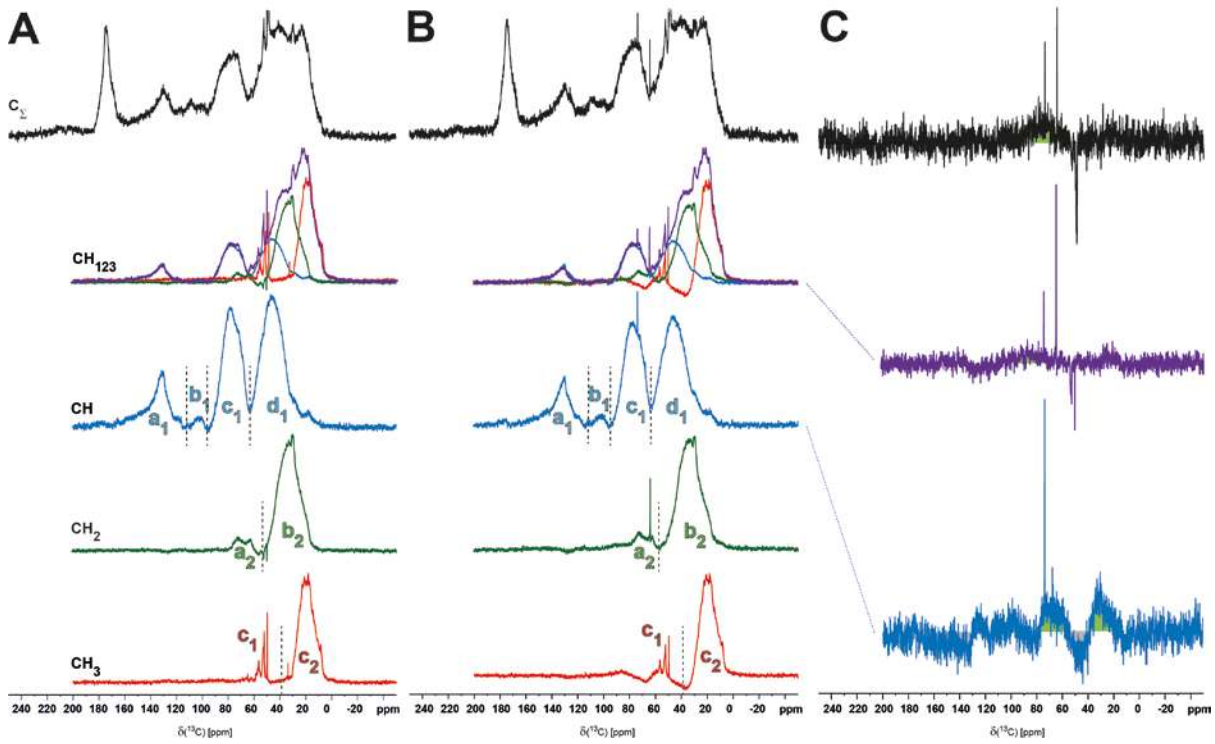

Figure S2: ^{13}C NMR spectra of Raberga slow sand SPE-DOM ($^{12}CD_3OD$ solution, B_0 = 11.7 T) obtained by solid phase extraction (PPL) before (**A**) and after (**B**) chlorination; ^{13}C DEPT NMR spectra: (top) superimposed protonated carbon NMR resonances (CH_{123}; DEPT-45 ^{13}C NMR spectra), multiplicity-edited ^{13}C NMR spectra are (second from top) CH; methin, with indices a_1-d_1 denoting following chemical environments: H**C**$_{ar}$-C / O-H**C**-O / H**C**-O / H**C**-C), (second from bottom) CH_2; methylene, with indices a_2 and b_2 denoting following chemical environments: H_2**C**-O / H_2**C**-**C**, and (bottom) CH_3; methyl, with indices a_3 and b_3 denoting following chemical environments : H_3**C**-O / H_3**C**-C**.** The respective ^{13}C NMR section integrals are provided in Tab. 4. (**C**) difference ^{13}C NMR spectra as derived from (top) single pulse ^{13}C NMR spectra, (middle) DEPT-45 ^{13}C NMR spectra, and (bottom) DEPT-90 ^{13}C NMR spectra.